ARCHIVE OF MECHANICAL ENGINEERING

DOI: 10.24425/ame.2025.153741 2025, Vol. 72, No. 2, pp. 293–309

Yaroslav LYTVYNIAK [1], Vadym STUPNYTSKYY [1], Ihor YURCHYSHYN [1], Oksana LYTVYNIAK [1]

Modeling of hardening and burnishing of workpiece surfaces by toroidal impact indenter

Received 10 November 2024, **Revised** 7 April 2025, **Accepted** 24 April 2025, **Published online** 12 May 2025

Keywords: indentation, hardening, impact indenter, indentation depth, elasto-plastic half-space

The formation of the operational characteristics of parts is contingent upon the quality indicators of the surface and sub-surface layers of the workpieces. This process is primarily accomplished during the final stages of production. The hardening of the surface of the parts using cold plastic deformation ensures the operational characteristics of the machine parts. Dynamic hardening processes are highly effective compared to other hardening and burnishing processes used on workpiece surfaces. To utilize the advantages of the impact hardening method, it is necessary to determine the influence of the principal technological parameters on the anticipated quality characteristics of the surface layer of the workpiece. This article presents the results of theoretical research of the process of contact dynamic deformation of a workpiece surface by a toroid-peen rigid indenter with a free or elastic connection. The dependencies were obtained to determine the maximum contact force, the values of the maximum elastic and plastic indentation, the parameters of the indentation contour, and the thickness of the hardened surface layer of the workpiece, which are dependent on the speed, the geometric dimensions of the contact workpiece of the toroidal indenter, and the elastic and plastic characteristics of the workpiece materials for indenters with a free and elastic connection. The study concentrated on the significance of establishing the duration of the active indentation phase, which occurs with an increase in the applied force, and the duration of the passive indentation phase, which occurs with a decrease in the applied force. The utilization of an elastic connection with defined characteristics, which are incorporated into the indenter, will prolong the duration of the passive indentation phase.

✉ Vadym STUPNYTSKYY, e-mail: Vadym.V.Stupnytskyi@lpnu.ua

[1] Lviv Polytechnic National University, Lviv, Ukraine

1. Introduction

One of the main features of modern production is ensuring the required quality of products. It is determined by the corresponding geometric, physical, and mechanical characteristics of individual parts achieved during the finishing machining process. The procedures during the machining process of workpieces are accompanied by residual changes and surface integrity in the sub-surface layer, e.g., surface roughness, microhardness, and residual stresses. The integrity of the workpiece surface and sub-surface layers affects the parts' functional characteristics as resistance to wear, fatigue, strength, etc. Therefore, ensuring the operational functions of parts is especially important when the machining process of modern metal alloys in the automotive, energy, aerospace, and other industries is carried out [1, 2]. The finishing process methods are being developed and implemented to reduce the influence of formed surface defects during the machining process on the functional characteristics of products because these methods reduce or eliminate the mentioned damages.

One of the most effective technological methods for replacing expensive superfinishing cutting methods (honing, finishing grinding, etc.) is the use of surface plastic deformation. The application of such technological operations has numerous advantages, including strengthening the workpiece's surface layer, creating a regular relief of the processed surface, and reducing the cost of expensive tools. The mathematical formalization of surface deformation is a complex process that affects the quality and adequacy of such technological operations' modeling. This article addresses this issue.

2. Literature review

The machining process effectively ensures the required operational functions of parts due to the obtaining appropriate quality characteristics of surfaces and sub-surface layer of workpieces. This process is based on the methods of hardening metal surfaces by plastic deformation [1–23].

The various hardening methods by surface plastic deformation are effectively used in mechanical engineering. These methods differ in the tool design and the scheme of its power load. The hardening of the surfaces of workpieces by plastic deformation is accompanied by structural changes in the sub-surface layer, reflected by the thickness of the strengthened metal layer, the value of residual stresses, and an increase in hardness [1–3].

Hardening methods of machined workpieces and burnishing processes stand out on the surface. Based on the ball burnishing method, a new burnishing process was developed in [5]. This process consists of imposing oscillating micromovements on the ball with the application on the outer or inner cylindrical surface, or the end surface. Such actions ensure a reduction in roughness, an increase in the hardness of the processed surface, and an increase in the effective performance

characteristics of workpieces [5]. Process roller burnishing and new slide roller burnishing are used to achieve smoothing, hardening, and mixed burnishing. The last new process ensures improvement by 42% smaller height roughness parameters and improvement by 7% a higher surface microhardness on the surface of AISI 316 steel than the first traditional roller burnishing [6]. The roller burnishing process has widespread applications. The use of a roller burnishing process for surface treatment of aluminum matrix composites reinforced with SiC particles allows the creation of smooth surfaces with considerable compressive residual stresses in the matrix alloy [10]. Moreover, this process can be used for the wear surface treatment of cast duplex steel workpieces to improve wear resistance [11]. It is worth noting that the assistance of ultrasonic vibrations on the ball burnishing process improved the average roughness by 2.9%, increased the von Mises stress at the surface by 11.5%, and increased the wear resistance of the 316L steel shaft to 7.3% [12].

Pulsed mechanical surface treatment achieves significant advantages in hardening workpiece surfaces. These are processes based on the phenomenon of mechanical impact. They include shot peening, deep rolling and machine hammer peening, microparticle bombarding, centrifugal shot peening, and vibration centrifugal treatment. Application of these processes has the following results: increasing the hardness of the surface and subsurface layers, improvement of surface micro-relief characteristics, obtaining residual compressive stress for metals, providing modification, integrity and surface hardening of cermet material and titanium alloys, improving the characteristics of processed welds in welded joints with reduced crack formation, increasing the safety operation with limited service life, in particular aero engine compressor disks, reducing the risk of failure by 11.31%, ensuring the performance characteristics of such workpieces as boring pipes and nipples connecting them for oil and gas drilling equipment [13–23].

The phenomenon of mechanical impact is used in a modified form by imparting an impulse load to the working element with a spherical surface of the tool from an additional machine hammer peening. This surface treatment process allows the effective applying plastic indentations on the practical surface and ensures sufficient hardness of the workpiece. It ensures residual compressive stress, finely dispersed metal structure, surface roughness that is close to operational roughness, and geometrically defined micro-relief that holds lubricant on the surface [4].

The dynamic hardening mechanical surface treatment process, which uses contact interaction upon impact of the working element – the indenter – with the treated surface of the part, is one of the energy-efficient processes of surface plastic deformation. For the practical use of its advantages, complete determinism of the processing results from the main technological parameters of the process is required. Therefore, it is relevant to develop recommendations for predicting the main characteristics of the quality of the part's surface layer. These characteristics can be established by determining the value of the maximum contact force of impact with a tool – an impact toroidal indenter on the elasto-plastic surface of the part, depending on the initial speed of the indenter and the elasto-plastic characteristics

of the workpiece material. The existing calculation models require improvement since they do not consider the tool design, the shape and geometric dimensions of the indenter, and the technological modes and conditions of the surface impact hardening treatment process [4, 7–9].

3. Research methodology

Surface plastic deformation treatment is used at the final stage of the technological process of workpiece production to reduce the surface roughness of the workpiece and harden and improve the material characteristics of the sub-surface layer of the part. Methods of surface plastic deformation are characterized by the absence of the part's material cutting. These methods can be static and dynamic depending on the action time criterion of the applied force to the deforming tool. Dynamic methods include the methods that use the physical phenomenon of impact of two bodies, i.e., a separate working element of the tool impacts the treated surface of the part. By design, the working elements of the tools can be either balls or rollers (discs). The working elements, for example, rollers (disks), can have a toroidal tip. The processed surface of the workpiece has the shape of a plane or a cylinder. The tool working element's impact on the part's processed surface is applied at a speed created by different methods [4, 7, 8, 21–23].

The rotational method of providing the tool working elements with an initial speed, when the tool rotates at a constant speed, is characterized by ease of implementation, controllability, and efficiency [7, 8]. The tool body is located at a distance from the processed workpiece surface. The working elements (indenters) are located in the tool body. Moreover, they rotate together with the tool body. They also alternately impact the processed workpiece surface, leaving residual indentations on this surface. These indentations correspond to the tip shape of the working element (indenter). The dimensions of the residual indentation depend on the kinetic energy of the indenter and the workpiece material properties. They determine the hardening values, internal residual stresses, and roughness parameters for the processed surface of the part. The depth of the residual indentation is determined by the force-deformation dependence during the contact interaction of the indenter with the workpiece surface [7–9, 24, 25]. The primary goal of this work is to determine the dependence between the indentation depth of the indenter into the workpiece material with elasto-plastic properties and the contact force, which arises during the impact process, considering the connection of the indenter with the body of the rotary tool.

The solution to this task is carried out using hypotheses about the independence and sequence of the elastic and plastic indentation of the indenter into the elasto-plastic half-space. Also, the identity of the dependences between contact forces and indentation depths under static and dynamic loads was included, considering changes in the mechanical properties of the material [9, 24, 25]. The diagram of indentation depth – force indentation load – force indentation unload is shown

in Fig. 1. 0AE is the indenter load line during the elastic indentation; P_0B is the indenter load line during the plastic indentation; 0AD is the indenter load line during the elasto-plastic indentation; DC is the indenter unloading line (force reduction) during elastic recovery of the indentation. P_m is the maximum force of elasto-plastic contact indentation; P_k is the intermediate force of elasto-plastic contact indentation; P_0 is the force at which plastic deformation begins at the center of contact. h_0 is the limit indentation of the indenter into the elastic half-space before the onset of plastic deformation; h_k is the general elasto-plastic indentation of the indenter into the half-space under the action of force P_k; h_{rk} is the elastic indentation of the indenter into the half-space under the action of force P_k; h_{pk} is the plastic indentation of the indenter into the half-space under the action of force P_k; h_m is the general elasto-plastic indentation of the indenter into the half-space under the action of force P_m; h_r is the elastic indentation of the indenter into the half-space under the action of force P_m; h_p is the plastic indentation of the indenter into the half-space under the action of force P_m.

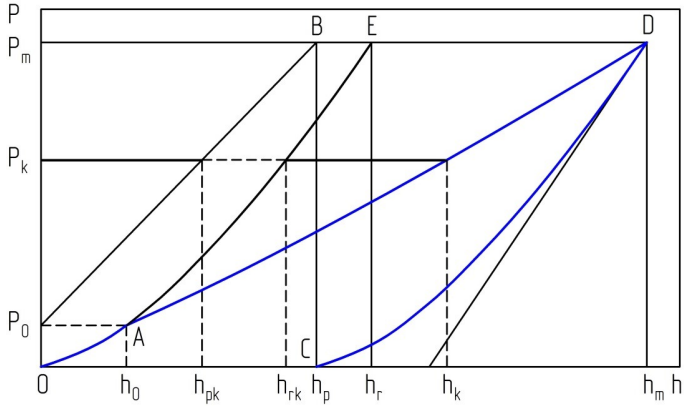

Fig. 1. Diagram of the contact kinetic indentation of the rigid ball indenter into the elasto-plastic half-space

The general indentation of the indenter h_k into the elasto-plastic half-space under the action of a force applied to the indenter P_k consists of successive elastic and plastic indentations if the forceP_k is greater than the force for the occurrence of plastic deformation P_0 ($P_k > P_0$):

$$h_k = h_{rk} + h_{pk}. \tag{1}$$

The indentation of a rigid indenter with a spherical tip into an elastic half-space, depending on the contact force P_k, can be established using Hertz's law (we consider that the elastic properties of materials remain practically unchanged, at least up to an indentation speed of 10 m/s) [7–9, 24, 25]:

$$h_{rk} = k_r P_k^{2/3}, \tag{2}$$

where k_r is the coefficient that considers the elastic mechanical properties of the indenter and workpiece material and the geometric parameters of their surfaces in contact.

The coefficient k_r is determined using the known relationship:

$$k_r = \left(\frac{9\pi^2}{16} \frac{1}{R_{eff}} \left(\frac{1-\nu_1^2}{\pi \mathrm{E}_1} + \frac{1-\nu_2^2}{\pi \mathrm{E}_2} \right)^2 \right)^{1/3}, \tag{3}$$

where ν_1, ν_2 are the Poisson's ratios; E_1 is Young's modulus of the indenter material; E_2 is Young's modulus of the workpiece material; R_{eff} is the effective radius of the indenter's curvature and the workpiece surface:

$$R_{eff} = \left(\left(\frac{1}{R_{11}} + \frac{1}{R_{12}} \right) \left(\frac{1}{R_{21}} + \frac{1}{R_{22}} \right) \right)^{-1/2}, \tag{4}$$

where R_{ij} are the radii of curvature of the contacting body's surfaces (i, j – respectively, the curvature plane number, and the indenter and the part).

Depending on the force P_k, the component of the deepening of a rigid spherical indenter into a plastic half-space in contact is determined by a linear dependence, confirmed experimentally under dynamic loads and described by a modified formula [7–9, 24]:

$$h_{pk} = k_p (P_k - P_0), \tag{5}$$

where k_p is the coefficient that considers the effective radius of the indenter's curvature, the workpiece surface, and the plastic properties of the workpiece material, which depends on the indentation speed.

The coefficient k_p is determined by the equation:

$$k_p = (2\pi R_{eff} \eta H_P)^{-1}, \tag{6}$$

where H_P is the value of static plastic hardness of the workpiece material in the initial state, MPa; η is the dynamic plastic hardness coefficient.

When describing the hardening parameters of the surfaces of the workpieces under dynamic loads with an indenter, it is necessary to use the characteristics of the workpiece material that differ from those obtained under static loads; for example, dynamic plastic hardness is ηH_P.

A connection has been established between the values of plastic hardness and the Brinell hardness of the material [7, 9]:

$$H_P = (23/49)\mathrm{HB}^{100/89}, \tag{7}$$

where HB is Brinell hardness of the workpiece material, MPa.

Using results of experimental studies [9], obtained for various structural and alloy steels, for example steel C22, C45, 41Cr4, 30CrMnSiA, we received empirical

dependencies for determining the force of plastic deformation onset P_0 at the center of the indenter contact with the part's surface and dynamic plastic hardness coefficient η (parameters change limits are P_0: (8–2210), N; H_P: (1000–8000), MPa; V: (1–10), m/s; η: (1.18–1.95); V/H_P: $(4.25 \cdot 10^{-4} - 6.94 \cdot 10^{-3})$, m MPa/s):

$$P_0 = \exp(100.168 - 0.294(\ln H_P)^3 + 6.656(\ln H_P)^2 - 46.995 \ln H_P), \quad (8)$$

$$\eta = 1.0887 + 248.96\left(\frac{V}{H_P}\right) - 18040\left(\frac{V}{H_P}\right)^2, \quad (9)$$

where V is the initial indentation speed, m/s.

4. Research results

The indentation process of a rigid indenter into an elasto-plastic half-space is determined based on expressions (Eq. 1, Eq. 2, and Eq. 5).

When the maximum contact load P_m is reached (active loading stage), we can obtain the maximum elasto-plastic indentation of the indenter (Fig. 1), and it can be determined by the expression:

$$h_m = (h_r + h_p) = k_r P_m^{2/3} + k_p(P_m - P_0). \quad (10)$$

This expression consists of the maximum elastic indentation depth of indenter h_r and the maximum plastic indentation depth of indenter h_p. The maximum elastic indentation depth of indenter h_r is established by Hertz's law:

$$h_r = k_r P_m^{2/3}.$$

The passive unloading stage can be described using Hertzian dependence (Eq. 2), and elastic restoration of the elasto-plastic indentation occurs during this stage. This indentation decreases by the value h_r, and it is accompanied by the formation of a residual indentation with a depth that equals the size of the maximum plastic indentation h_p, which is described by the following expression:

$$h_p = k_p(P_m - P_0). \quad (11)$$

The maximum contact load P_m is the determining factor in calculating the residual plastic indentation h_p.

We will consider two cases of contact interaction of an indenter with an elasto-plastic half-space when impacting with a free indenter (the external connections are absent) and impact with an indenter with an external elastic connection.

4.1. Dynamic (impact) indentation of free rigid indent into elasto-plastic half-space

4.1.1. Active stage of indentation

The motion equation of the mass center of the indenter during the deformation of the half-space has the form:

$$m\frac{\mathrm{d}^2h}{\mathrm{d}t^2} = -P(h), \tag{12}$$

where m is the mass of the indenter; h is the elastic and elasto-plastic indentation of the indenter into the sub-surface layer of the part; t is the arbitrary point in time during the active stage of the impact (from 0 to t_a); $P(h)$ – variable contact force (function of the size of the contact indentation h).

Applying the typical procedure for solving Eq. 12 we receive:

$$E = \frac{mV^2}{2} = \int_0^{h_k} P_k(h)\,\mathrm{d}h, \tag{13}$$

where E is the initial kinetic energy of the indenter before the impact; V is the initial speed of the mass center of the indenter at the moment of contact with the half-space.

Successful solution of the Eq. 13 is possible when the expression $P_k = P_k(h)$ is deterministic. Besides that, the indentation force P_k is a function of the variable indentation depth h in the previous expression.

The ratios Eq. 2 , Eq. 5 and Eq. 1 establish a relationship $h = h(P_k)$, in which the size of indentation h is a function of the load force on the indenter P_k.

Using the interpretation of the definite integral I_1 as the value of the area bounded by the line and the h-axis from the right side of Eq. 13, we get:

$$I_1 = \int_0^{h_k} P_k(h)\,\mathrm{d}h = P_k h_k - \int_0^{P_k} h(P_k)\,\mathrm{d}P_k =$$

$$= P_k h_k - \left[\int_0^{P_0} k_r P_k^{2/3}\,\mathrm{d}P_k + \int_{P_0}^{P_k} \left(k_r P_k^{2/3} + k_p(P_k - P_0)\right)\mathrm{d}P_k\right].$$

Considering Eq. 1, Eq. 2, and Eq. 5, we get: $P_k h_k = P_k(k_r P_k^{2/3} + k_p(P_k - P_0))$.

Solving Eq. 13, considering previous expression, we establish a connection between the initial kinetic energy of the indenter E and the maximum indentation force P_m, considering the elastic and plastic characteristics of the workpiece material:

$$E = \frac{mV^2}{2} = \frac{2}{5}k_r P_m^{5/3} + \frac{1}{2}k_p(P_m^2 - P_0^2). \tag{14}$$

The previous expression indicates that the total kinetic energy of the rigid indenter E is converted into the energy of elastic recoverable deformation of $\frac{2}{5}k_r P_m^{5/3}$ and plastic residual deformation of $\frac{1}{2}k_p(P_m^2 - P_0^2)$ of the elasto-plastic half-space.

Expression 14 is the transcendental equation for determining P_m (P_m is the maximum impact force of the indenter on the elasto-plastic half-space). After transformations, we obtain an expression for determining P_m by the method of successive approximations (simple iterations):

$$P_m = \left[\frac{2E + k_p P_0^2}{\frac{4}{5}k_r P_m^{-1/3} + k_p}\right]^{1/2}. \tag{15}$$

The maximum value of the indenter's elasto-plastic indentation hm and residual plastic indentation h_p of the indenter is determined by the value of P_m according to Eq. 10 and Eq. 11.

To determine other characteristics of the active stage of the impact process, in particular, its duration, it is advisable to approximate the expression Eq. 15 by power-law dependence in the form:

$$P_k = b h_k^n, \tag{16}$$

where b and n are the coefficient and exponent, respectively.

The approximation is carried out based on the following prerequisites: the function graph Eq. 16 passes through a point with coordinates (h_m, N_m) and the areas are limited by the functions graphs Eq. 14 and Eq. 16 are the same, i.e., the line 0AD in Fig. 1 is replaced by a single line corresponding to Eq. 16.

According to the first condition, we can determine $P_m = b h_m^n$. We can use Eq. 13 and Eq. 16 to satisfy the second condition. After integration, we get: $E = \frac{b}{n+1} h_m^{n+1}$.

Using Eq. 15 and Eq. 10, we can determine P_m and h_m and we must substitute the determined values E in Eq. 16 to determine the parameters b and n:

$$n = \frac{h_m P_m}{E} - 1, \quad b = P_m h_m^{-n}. \tag{17}$$

Considering that the variable speed of the indenter depth into the workpiece surface is equal $V = \frac{\mathrm{d}h}{\mathrm{d}t}$ and using Eq. 16, we get:

$$\left(\frac{\mathrm{d}h}{\mathrm{d}t}\right)^2 = V^2\left(1 - \frac{1}{E}\frac{b}{n+1}h_k^{n+1}\right) = V^2\left(1 - \left(\frac{h_k}{h_m}\right)^{n+1}\right).$$

The duration of the active stage of indentation t_a can be determined by integrating the previous expression from $t = 0$ to $t = t_a$ and using dependences $h_k = 0$ and $h_k = h_m$:

$$t_a = \frac{h_m}{V}\sqrt{\pi}\left(\frac{1}{2} + \frac{E}{h_m P_m}\right)\frac{\Gamma\left(\frac{1}{n+1}\right)}{\Gamma\left(\frac{1}{n+1} + \frac{1}{2}\right)}, \tag{18}$$

where Γ is the Gamma function.

4.1.2. Passive stage of indentation

The passive indentation stage occurs when the indenter's applied force decreases. This stage is accompanied by the action of elastic deformations that cause a decrease in the indentation depth, which was obtained at the active stage of the elasto-plastic indentation.

The residual plastic indentation h_p corresponds to the value of the maximum plastic deformation. Hertz's law describes the elastic restoration of an indentation.

The variable value of the decreased indentation of the indenter (it corresponds to the DC line in the diagram Fig. 1) can be determined by the expression:

$$h_k = (h_{rk} + h_p) = k_r P_k^{2/3} + h_p.$$

The value of the contact force of the indenter with the elasto-plastic half-space is described using dependence:

$$P_k = \left(\frac{1}{k_r}(h_k - h_p)\right)^{3/2}.$$

The motion differential equation of the indenter mass center during the passive stage has the form:

$$\frac{\mathrm{d}^2 h}{\mathrm{d}t^2} = -\frac{1}{m}P(h) = -\frac{1}{m}\left(\frac{1}{k_r}(h_k - h_p)\right)^{3/2}. \tag{19}$$

Solution to Eq. 19 allows us to determine the movement speed of the indenter at the moment when the contact between the indenter and the workpiece surface disappears and then the post-impact kinetic energy of the indenter E_1:

$$E_1 = \frac{mV_m^2)}{2} = \frac{2}{5}k_r^{-3/2}P_m^{5/3}, \tag{20}$$

where V_m is the post-impact speed of the indenter mass center.

The duration t_p of the passive stage of the impact can be determined from following equation by applying the considerations used when obtaining Eq. 18:

$$t_p = \frac{2}{5}\frac{h_r}{V_m}\sqrt{\pi}\frac{\Gamma\left(\frac{2}{5}\right)}{\Gamma\left(\frac{9}{10}\right)}. \tag{21}$$

After appropriate transformations, which consists in determining from expression 20 the value of the post-impact speed V_m and the numerical values of the Gamma function, the expression for determining the duration t_p of the passive stage of the indenter impact on an elasto-plastic half-space takes the following form:

$$t_p = 1.878925\sqrt{k_r}\sqrt{m}P_m^{-1/6}. \tag{22}$$

4.2. Dynamic (impact) indentation of a rigid indenter with an external elastic connection into an elasto-plastic half-space

Dynamic (impact) deformation of the half-space surface (Fig. 2) is carried out by a rigid indenter with a toroidal surface connected to an elastic element.

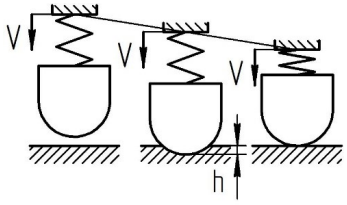

Fig. 2. The indentation scheme of the rigid indenter with elastic connection into the elasto-plastic half-space

The movement of the indenter is ensured by the movement of the elastic element, the base of which moves uniformly progressively at a constant speed V during the active and passive stages of impact indentation. The base of the elastic element will move a distance S_a during the active stage of the impact (its duration is t_a). The base of the elastic element will move a distance S_p during the passive stage of the impact (its duration is t_{ep}). We use the following preconditions for the calculation. During the active stage of the indenter depth, the base of the elastic element S_a will move a distance, which is equal to the maximum depth of the elasto-plastic indentation h_m, that is, there is no deformation of the elastic element. Consequently, the active stage of the indentation of a rigid indenter with an elastic connection is similar to the indentation of a free rigid indenter established by Eq. 12 and Eq. 14. During the duration of passive impact stage t_{ep}, the base of the elastic element will move by the value of the maximum elastic indentation of the indenter h_{er}, and the indenter will move a variable distance that is equal to

$(h - h_{ep})$. Consequently, during the passive stage of indentation, the total value of deformation of the elastic element is equal to $(h_{er} + h - h_{ep})$. We assume that the total mass of the indenter me is equal to the mass of the free indenter m and the mass of the elastic element m_c, i.e., $m_e = m + m_c$.

The differential equations for the movement of the mass center of a toroidal indenter with an elastic connection during the indentation of an elasto-plastic half-space, respectively, for the active and passive stages of impact, are as follows:

$$m_e \frac{\mathrm{d}^2 h}{\mathrm{d}t^2} = -P(h), \tag{23}$$

$$m_e \frac{\mathrm{d}^2 h}{\mathrm{d}t^2} = -P(h) + C(h_r + h_m - h), \tag{24}$$

where C is the elastic element rigidity, N/m.

We can solve the Eq. 23 and Eq. 24 using the statements by which we solved Eq. 12 and Eq. 19.

4.2.1. Active stage of indentation

The maximum indentation force P_{em}, the maximum elasto-plastic indentation depth h_{em}, the maximum elastic indentation depth h_{er}, the maximum residual elastic indentation depth h_{ep}, and the duration of the active impact stage by an indenter t_{ea} with an elastic connection are determined from Eqs. 15, 10, 11 and 18, considering that the mass m is equal to the total mass of the indenter m_e.

4.2.2. Passive stage of indentation

The kinetic energy of the indenter after impact $E_{1e} = \dfrac{m_e V_m^2}{2}$, which can be used to calculate the speed of the indenter after impact V_m, is given by Eq. 25. Using Eq. 25 we must consider the reasoning which was used to establish the expression 20. The kinetic energy of the indenter after impact depends on the maximum elastic indentation depth of the indenter h_{er} at the active stage of indentation and it can be determined:

$$E_1 e = \frac{m_e V_m^2}{2} = \frac{2}{5} k_r^{-3/2} h_{er}^{5/2} - \frac{3}{2} C h_{er}^2,$$

or

$$E_1 e = \frac{m_e V_m^2}{2} = \left(1 - \frac{15}{4} C k_r P_{em}^{-1/3}\right) \frac{2}{5} k_r P_{em}^{5/3} \tag{25}$$

The duration of the passive stage of the impact t_{ep} will be determined by integrating the Eq. 26, using the approach to determine the duration of the stages of

elasto-plastic indentation for a free indenter, reflected in determining the dependencies Eqs. 18, 21, using the right side of Eq. 24:

$$t_{ep} = \int_{h_{er}}^{0} \frac{m_e^{1/2}\,\mathrm{d}h}{\sqrt{\frac{4}{5}k_r^{-3/2}\left(h_{er}^{5/2} - h^{5/2}\right) + C\left(2h_{er}h + h^2 - 3h_{er}^2\right)}}. \tag{26}$$

It is advisable to perform the determination t_{ep} by numerically integrating Eq. 26.

The duration of the passive and active stages of the indenter's contact with the workpiece surface can be used to influence the efficiency of the machining process by increasing the duration of the force in contact with the expected increase in the duration of the passive stage of the indenter's impact with an elastic connection.

4.3. The hardening parameters of workpiece surface layer

The established value of the maximum indentation force P_m, together with the dimensions of the contact workpiece of the toroidal indenter, allows us to determine the dimensions of the contour of the residual plastic indentation on the workpiece surface and the thickness of the hardened layer using [8, 9].

The dimensions of the residual indentation, which is elliptical in plan, are determined by the semi-axes a and b, which are defined by the formulas:

$$a = \left((h_m + h_p)R_{11} - h_p^2\right)^{1/2}; \quad b = \left((h_m + h_p)R_{12} - h_p^2\right)^{1/2}, \tag{27}$$

where R_{11} and R_{12} are radii of curvature of the contact surface of a toroidal indenter.

The indentation depth of plastic deformations f_p, which corresponds to the thickness of the hardened layer of the workpiece material, is calculated using the following expression:

$$f_p = \left(1 - \frac{1}{2}\left(1 - \frac{b}{a}\right)^4\right)\left(\frac{2P_m}{\eta H_P}\right)^{1/2}. \tag{28}$$

The parameters of the surface treatment of the part are directly influenced by the maximum impact force of the indenter P_m, the value of which depends on the hardness of the workpiece surface H_P and the initial speed of the mass center of the indenter V, which is shown in Fig. 3. This influence is reflected for steels C22 (H_P = 1440 MPa), 41Cr4 (H_P = 2530 MPa) and 30CrMnSiA (H_P = 4710 MPa) for an indenter with a mass m = 0.05 kg and the effective radius of the indenter R_{eff} = 0.005 m.

The influence of the value of static plastic hardness of the workpiece material H_p on the hardening parameters of the workpiece surface layer has different features, which is shown in Fig. 4. During the increase of the value of static plastic

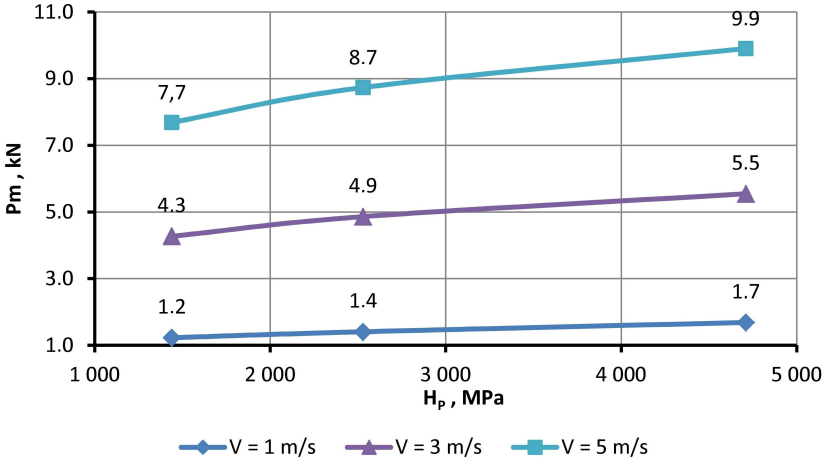

Fig. 3. Influence of the value of static plastic hardness of the workpiece material H_p on the maximum impact force of the indenter P_m

hardness H_p, the elastic indentation h_r increases, but the plastic indentation h_p decreases. In Fig. 4 there is presented: line 1, line 3 and line 5 – the elastic indentation h_r; line 2, line 4 and line 6 – the plastic indentation h_p; line 1 and line 2 the initial speed of the indenter $V = 1$ m/s, line 3 and line 4 the initial speed of the

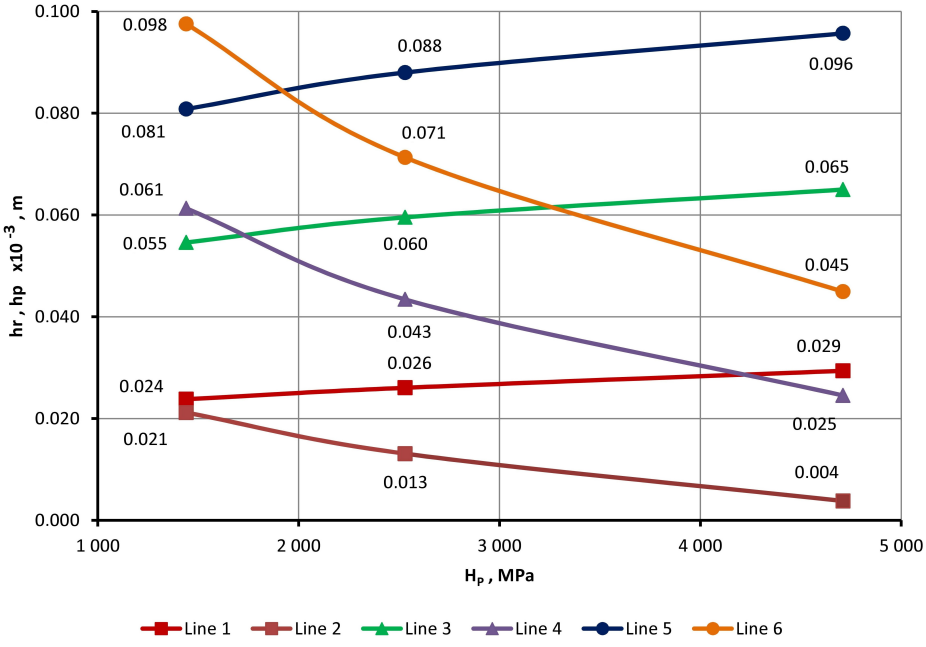

Fig. 4. Influence of the value of static plastic hardness of the workpiece material H_p on the elastic indentation h_r and the plastic indentation h_p

indenter $V = 3$ m/s, line 5 and line 6 the initial speed of the indenter $V = 5$ m/s; the mass of the indenter is $m = 0.05$ kg and the effective radius of the indenter – $R_{eff} = 0.005$ m; steel classes and their hardness are used as for Fig. 3.

5. Conclusions

- The simulation of the process of dynamic surface elasto-plastic treatment of a workpiece reflects the influence of three principal production factors: the movement speed of the mass center of the toroidal indenter, the dimensions of the contact surface of the indenter (with radii of curvature ranging from 1–5 mm to 10–20 mm) and the elasto-plastic characteristics of the workpiece material, the surface of which is subject to hardening and burnishing.
- The hardening and burnishing process of workpiece surfaces by toroidal impact indenter is characterized by different influences on the initial values of hardening parameters of the workpiece surface layer. For steels, during a significant increase in the initial hardness of the workpiece surface, the expected elastic indentation increases, but the plastic indentation decreases. This tendency increases with increasing initial indenter speed. The elastic indentation can be expected to be three times bigger than the plastic indentation.
- The dimensions of the toroidal indenter's contact surface significantly influence the maximum impact force. Furthermore, a reduction in the effective radius of curvature of the indenter allows the kinetic energy to be distributed more efficiently, resulting in the formation of a plastic indentation at a lower speed. This enables the same hardness level to be achieved with less energy expenditure. The rigidity of the elastic element exerts an influence on the parameters of surface plastic deformation, which in turn gives rise to a reduction in the post-impact speed for an indenter with an elastic connection. The utilization of an indenter with an elastic connection is of practical significance. The spread speed of plastic deformation in elasto-plastic materials is slower than that of elastic deformation. Consequently, increasing the duration of the passive stage of elasto-plastic indentation will result in an increase in the duration of action of the contact force and an enhancement in the efficiency of the hardening process.
- It is recommended to carry out design and technological modeling of surface hardening and burnishing processes using impact toroidal indenters according to the methods described in the article to determine the maximum impact indentation force, approximate the dependencies for the indentation diagram, and determine the dependencies for the elastic and dynamic characteristics of structural materials.

References

[1] Z. Liao et al. Surface integrity in metal machining – Part I: Fundamentals of surface characteristics and formation mechanisms. *International Journal of Machine Tools and Manufacture*, 162:103687, 2021. doi: 10.1016/j.ijmachtools.2020.103687.

[2] Z.M. Odosii, V.Ya. Shimanskyi, and B.V. Pindra. Influence of reinforcing plastic surface deformation on surface performance of machine parts. *Scientific Bulletin of Ivano-Frankivsk National Technical University of Oil and Gas*, 2(47):7–14, 2019. doi: 10.31471/1993-9965-2019-2(47)-7-14. (in Ukrainian).

[3] I. Gunko and M. Paladiy. Evaluation of the plasticity of the surface layer of metal during rolling of cylindrical parts with a ball. *Journal of Mechanical Engineering and Transport*, 15(1):58–66, 2022. doi: 10.31649/2413-4503-2022-15-1-58-66. (in Ukrainian).

[4] M.M. Kosiyuk and S.A. Kosttyuk. Increasing the efficiency use impact energy at static – pulsed surface plastic strengthening. *Herald of Khmelnytskyi National University*, 4(263):48–55, 2018. (in Ukrainian).

[5] V. Dzyura, P. Maruschak, S. Slavov, D. Dimitrov, V. Semehen, and O. Markov. Evaluating some functional properties of surfaces with partially regular microreliefs formed by ball-burnishing. *Machines*, 11(6):633, 2023. doi: 10.3390/machines11060633.

[6] J. Maximov, G. Duncheva, A. Anchev, V. Dunchev, K. Anastasov, and P. Daskalova. Effect of roller burnishing and slide roller burnishing on surface integrity of AISI 316 steel. Theoretical and experimental comparative analysis. *Machines*, 12(1):51, 2024. doi: 10.3390/machines12010051.

[7] A. Dudnikov, A. Kelemesh, and O. Gorbenko. Improving the technology of part machining by surface plastic deformation. *Eastern-European Journal of Enterprise Technologies*, 6(1)(102):26–32, 2019. doi: 10.15587/1729-4061.2019.183541.

[8] A.P. Minakov, Technology of finishing strengthening pneumo-vibro-dynamic processing of non-rigid parts, *Belorussko-Rossijskij Universitet*, 2016. (in Russian).

[9] M.M. Matlin, et al. Methods for non-destructive testing of the strength properties of machine parts. *Innovative Mechanical Engineering*, 247, 2019. (in Russian).

[10] A. Nestler and A. Schubert. Roller burnishing of particle reinforced aluminium matrix composites. *Metals*, 8(2):95, 2018. doi: 10.3390/met8020095.

[11] G. Stradomski, J. Fik, Z. Lis, D. Rydz, and A. Szarek. Wear behaviors of the surface of duplex cast steel after the burnishing process. *Materials*, 17(8):1914, 2024. doi: 10.3390/ma17081914.

[12] E. Velázquez-Corral, V. Wagner, R. Jerez-Mesa, J. Lluma, J.A. Travieso-Rodriguez, and G. Dessein. Analysis of ultrasonic vibration-assisted ball burnishing process on the tribological behavior of AISI 316L cylindrical specimens. *Materials*, 16(16):5595, 2023. doi: 10.3390/ma16165595.

[13] D. Meyer, M. Hettig, and N. Mensching. Pulsed mechanical surface treatment – an approach to combine the advantages of shot peening, deep rolling, and machine hammer peening. *Journal of Manufacturing and Materials Processing*, 5(3):98, 2021. doi: 10.3390/jmmp5030098.

[14] X. Xie, L. Zhang, L. Zhu, Y. Li, T. Hong, W. Yang, and X. Shan. State of the art and perspectives on surface-strengthening process and associated mechanisms by shot peening. *Coatings*, 13(5):859, 2023. doi: 10.3390/coatings13050859.

[15] Fu-Chuan Hsu, et al. The process parameters of Micro Particle Bombarding (MPB) for surface integrity enhancement of cermet material and tool steel. *Micromachines*, 14(3):643. 2023. doi: 10.3390/mi14030643.

[16] K. Gao, Y. Zhang, J. Yi, F. Dong, and P. Chen. Overview of surface modification techniques for titanium alloys in modern material science: a comprehensive analysis. *Coatings*, 14(1):148, 2024. doi: 10.3390/coatings14010148.

[17] R. Kosturek, T.Ślęzak, J. Torzewski, M. Bucior, W. Zielecki, L. Śnieżek, and J. Sęp. Effect of shot peening on the low-cycle fatigue behavior of an AA2519-T62 friction-stir-welded butt joint. *Materials*, 16(22):7131, 2023, doi: 10.3390/ma16227131.

[18] G. Li, Y. Teng, and H. Zhou. Modified method for surface probabilistic risk assessment of aero engine compressor disks considering shot peening. *Aerospace*, 10(7):621, 2023. doi: 10.3390/aerospace10070621.

[19] Y. Lei, Z. Wang, and H. Qi. Strengthening performance optimization of single ball impact treatment by evaluating residual stress. *Materials*, 15(10):3719, 2022. doi: 10.3390/ma15103719.

[20] A. Skoczylas and K. Zaleski. Study on the surface layer properties and fatigue life of a workpiece machined by centrifugal shot peening and burnishing. *Materials*, 15(19):6677, 2022. doi: 10.3390/ma15196677.

[21] V. Schulze, F. Bleicher, P. Groche, Y.B. Guo and Y.S. Pyun. Surface modification by machine hammer peening and burnishing. *CIRP Annals*, 65(2):809–832, 2016. doi: 10.1016/j.cirp.2016.05.005.

[22] W.L. Chan and K.F. Cheng. Hammer peening technology – the past, present, and future. *International Journal of Advanced Manufacturing Technology*, 118:683–701, 2022. doi: 10.1007/s00170-021-07993-5.

[23] Z. Huda. Torsion in shafts. In: *Mechanical Behavior of Materials: Fundamentals, Analysis, and Calculations*. Cham: Springer, 2021. doi: 10.1007/978-3-030-84927-6_10.

[24] V.V. Kharchenko, O.A. Katok, R.V. Kravchuk, A.V. Sereda, and V.P. Shvets. Analysis of the methods for determination of strength characteristics of NPP main equipment metal from the results of hardness and indentation measurements. *Procedia Structural Integrity*, 36:59–65, 2022. doi: 10.1016/j.prostr.2022.01.003.

[25] H. Ghaednia, S.A. Pope, R.L. Jackson, and D.B. Marghitu. A comprehensive study of the elasto-plastic contact of a sphere and a flat. *Tribology International*, 93(A):78–90, 2016. doi: 10.1016/j.triboint.2015.09.005.